

Implementing an object-based multi-index protocol for mapping surface glacier facies from Chandra-Bhaga basin, Himalaya

Shridhar Digambar Jawak^{1,2}, Sagar Filipe Wankhede^{2,3,4*}, Alvarinho Joaozinho Luis², Prashant Hemendra Pandit⁵, Shubhang Kumar⁶

¹*Svalbard Integrated Arctic Earth Observing System (SIOS), SIOS Knowledge Centre, Svalbard Science Park, N-9171, Longyearbyen, Svalbard, Norway*

²*Earth System Science Organization (ESSO), National Centre for Polar and Ocean Research (NCPOR), Ministry of Earth Sciences (MoES), Govt. of India, Headland Sada, Goa 403804, India*

³*Department of Civil Engineering, Manipal Institute of Technology, Manipal Academy of Higher Education, Manipal, Karnataka 576104, India*

⁴*Department of Marine Geology, Mangalore University, Mangalagangothri, Karnataka 574199, India*

⁵*National Bureau of Soil Survey and Land Use planning (NBSS & LUP) - Indian Agriculture Research Institute (IARI), New Delhi 110012, India*

⁶*Centre for Land Resource Management, Central University of Jharkhand, Ranchi 835205, India*

Abstract

Surface glacier facies are superficial expressions of a glacier that are distinguishable based on differing spectral and structural characteristics according to their age and inter-mixed impurities. Increasing bodies of literature suggest that the varying properties of surface glacier facies differentially influence the melt of the glacier, thus affecting the mass balance. Incorporating these variations into distributed mass balance modelling can improve the perceived accuracy of these models. However, detecting and subsequently mapping these facies with a high degree of accuracy is a necessary precursor to such complex modelling. The variations in the reflectance spectra of various glacier facies permit multiband imagery to exploit band ratios for their effective extraction. However, coarse and medium spatial resolution multispectral imagery can delimit the efficacy of band ratioing by muddling the minor spatial and spectral variations of a glacier. Very high-resolution imagery, on the other hand, creates distortions in the conventionally obtained information extracted through pixel-based classification. Therefore, robust and adaptable methods coupled with higher resolution data products are necessary to effectively map glacier facies. This study endeavours to identify and isolate glacier facies on two unnamed glaciers in the Chandra-Bhaga basin, Himalayas, using an established object-based multi-index protocol. Exploiting the very high resolution offered by WorldView-2 and its eight spectral bands, this study implements customized spectral index ratios via an object-based environment. Pixel-based supervised classification is also performed using three popular classifiers to comparatively gauge the classification accuracies. The object-based multi-index protocol delivered the highest

Received May 27, 2019, accepted December 30, 2019.

*Corresponding author: S. F. Wankhede <swankhede436@gmail.com>

Acknowledgements: The authors thank Dr. Gangadhara Bhat, Chairman, Dept. of Geoinformatics, Mangalore University, and Dr. M. Ravichandran, Director ESSO-NCPOR for their motivation and support.

overall accuracy of 86.67%. The Minimum Distance classifier yielded the lowest overall accuracy of 62.50%, whereas, the Mahalanobis Distance and Maximum Likelihood classifiers yielded overall accuracies of 77.50% and 70.84% respectively. The results outline the superiority of the object-based method for extraction of glacier facies. Forthcoming studies must refine the indices and test their applicability in wide ranging scenarios.

Key words: Glacier facies, band ratios, object-based classification, customized spectral indices

DOI: 10.5817/CPR2019-2-11

Introduction

The transformation from snow to ice is not a linear change, but rather a continuously changing phenomenon. This implies that the factors contributing to the metamorphosis of fresh snow to its aged and varied forms are undergoing continuous change. These factors include precipitation, temperature, deposited particulates, debris cover *etc.* Meteorological fluxes in association with the surrounding geomorphology are the cause of the variations in the factors governing a glacier's life cycle (Benson 1962, Jawak *et al.* 2018a). The varied forms of snow and ice when localized on certain regions of a glacier create identifiable expressions. The characteristics of these expressions are differentiable from their surroundings. The distinct zones where the varied expressions are visible, usually correspond to the accumulation and ablation characteristics of the glacier and are called glacier facies (Paterson 1994). Over the surface of the glacier these facies intermix with natural/anthropogenic particles and can then be called surface glacier facies. Ali *et al.* (2017) observed the importance of understanding and assessing surface glacier facies as distinct zones having diverse melt rates and varying impacts on total deglaciation. This therefore implies that each facies provide varying contributions to the overall mass balance of the glacier. While Bamber *et al.* (2004) describes the investi-

gations of mass balance to be an extensive divulgence of glaciological processes, understanding the mass balance without incorporating surface glacier facies and their resultant effects invariably leave void sites in distributed mass balance models. An attempt at including facies in the 3-dimensional calibration of distributed models was made by Braun *et al.* (2007). Unfortunately, the duress of logistical and climatic constraints does not enable year-round in-situ facies data collection. Moreover, traditional methods for assessing mass balance focus on limited discharge rates and temperature, which inevitably leave out the 3-dimensional information of facies due to physical limitations of manual data collection.

Remotely sensed data, with its diverse applicability and year-round monitoring capacity is well placed to derive glacier facies and provide the necessary inputs to complex distributed mass balance modelling. Hence, the accuracy of the derived glacier facies is crucial to the resultant accuracy of the calibrated model. This accentuates the need for accurate information extraction techniques from the imagery. The use of multispectral satellite imagery for mapping glacier facies has been investigated through a variety of adaptive techniques (Hall *et al.* 1988, Heiskanen *et al.* 2002, Winsvold *et al.* 2016). Studies of snow and ice cover types begin from some

of the early investigations of the sensitivity of the visible and near infrared (NIR) spectrum to snow grain size and contamination (Dozier et al. 1981), as well as their resultant spectral characteristics in Landsat TM bands (Hall et al. 1988). Yousuf et al. (2019) analysed the effects of radiometric resolutions, the timing of acquisition and surface morphology on the derivable spectra of glacier facies in satellite imagery. Zhang et al. (2019) proposed an automatic algorithm for mapping ice cover types using multitemporal Landsat-8 imagery and multiple digital elevation models (DEMs). Tsai et al. (2019) used SAR data in conjunction with topographic supplemental inputs for mapping total snow cover and wet snow cover extent. Mapping of debris-covered glaciers has also been undertaken using a variety of methods usually involving singular or multiple satellite imageries coupled with a variety of ancillary inputs (Ali et al. 2017, Alifu et al. 2016, Shukla and Ali 2016, Bhardwaj et al. 2015, Bhambri et al. 2011). Even the object-based classification (OBC) approach is tested for its potential for mapping glaciers and glacial

covers (Jawak et al 2018a, b; Robson et al. 2015, Rastner et al. 2014) with impressive results. Numerous studies employ band ratioing either on the multispectral satellite imagery or for generation of ancillary inputs. While classification of image objects (OBC) instead of pixels has been used to utilize image spectra as well as contextual characteristics for, not only cryospheric mapping but also for other land cover mapping (Li et al. 2014), the efficiency of band ratioing techniques still hold their place in terms of exploiting spectral characteristics (Jensen 2015). An alliance of such band manipulations with OBC is therefore a window to uncharted potential capabilities.

Consequently, this study aims to utilize this potential for mapping the available range of glacier facies of two unnamed glaciers, located in the Chandra-Bhaga basin Himalayas. Using image classification as its base, this study tests the OBC technique by devising customized spectral index ratios and comparing it to the conventional pixel-based classification (PBC). The accuracy of the resulting classifications was estimated using error matrices.

Material and Methods

Study Area

The current study was performed on two selected glaciers in the Chandra-Bhaga basin, Himalayas. Administratively, they lie within the state of Himachal Pradesh, India (Fig. 1). The average elevation of this basin is around 4300 m. The two selected glaciers of the present study are not well monitored and as such have no officially designated names, therefore the global land ice measurement from space (GLIMS) reference number associated with the selected

glaciers are provided. This study refers to these glaciers as glacier A (GA) and glacier B (GB).

GA (GLIMS Id: G077368E32554N, Raup et al. 2007) is about 37.42 km² in area and GB (GLIMS Id: G077376E32671N, Raup et al. 2007) is about 27.70 km² in area. This basin is home to the Indian research base, Himansh, which is located beyond (on the Sutri Dhaka glacier) the extent of the imagery.

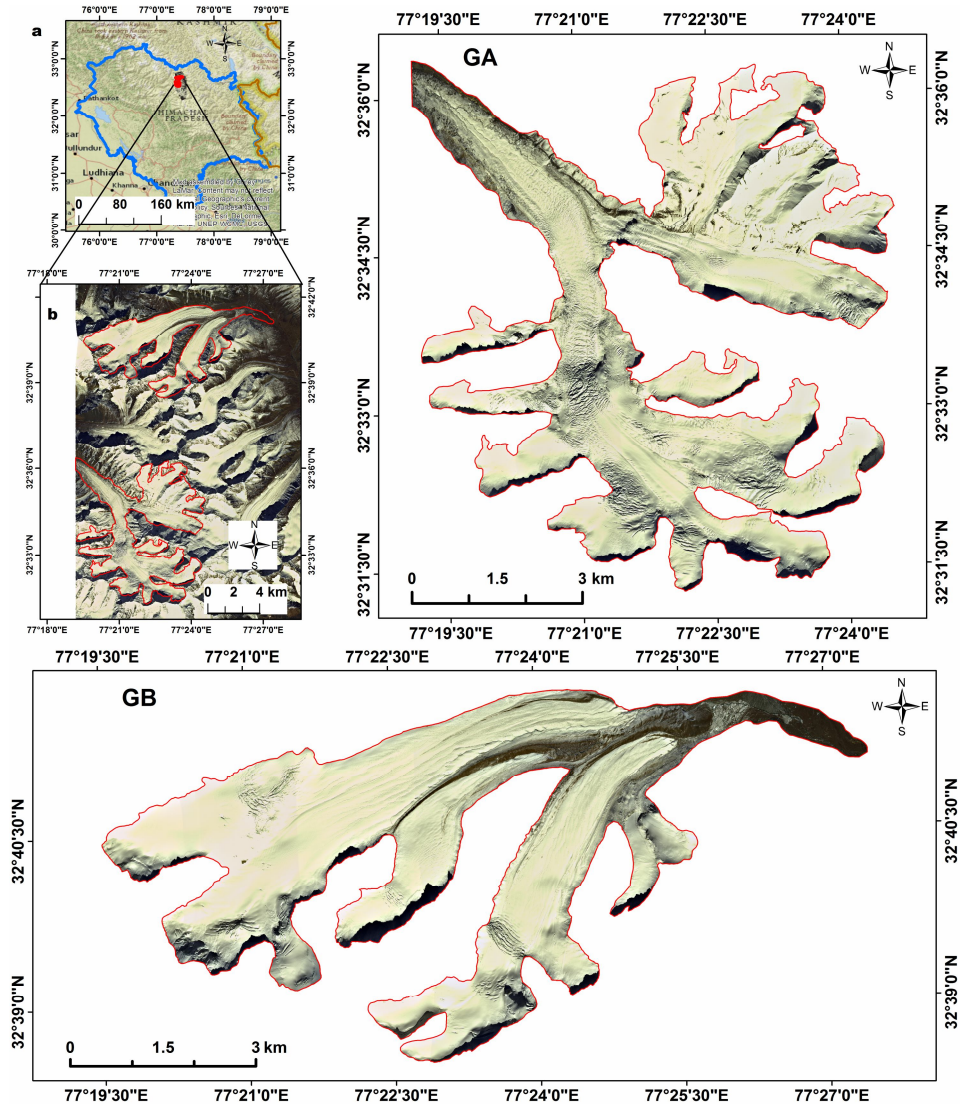


Fig. 1. Geographical location of the study area in the Chandra-Bhaga basin. Inset **a**: shows the administrative boundaries of the state of Himachal Pradesh (blue outline) over the national geographic baseline map. Inset **b**: shows the zoomed overview of glaciers GA and GB (red outlines) on the WorldView-2 imagery. GA and GB are the scaled up view of glaciers GA and GB respectively.

Data

The present study employs the Digital Globe's very high-resolution (VHR) World View-2 (WV-2) multispectral imagery. Armed with a multispectral spatial reso-

lution of 2 m and a panchromatic resolution of 0.5 m, this product can potentially identify minor features on the surface of a glacier that are often undetected

by coarser resolution imagery. The multi-spectral bandwidths of WV-2 comprise of coastal (0.40 – 0.45 μm), blue (0.45 – 0.51 μm), green (0.51 – 0.58 μm), yellow (0.565 – 0.625 μm), red (0.63 – 0.69 μm), red edge (0.705 – 0.745 μm), near infrared 1 (NIR1) (0.770 – 0.895 μm) and near infrared 2 (NIR2) (0.86 – 1.04 μm). The imagery was acquired on 16 October 2014, *i.e.* at the onset of winter. Jawak et al. (2018a and 2018b) have tested WV-2 for its capacity to map supraglacial facies.

Racoviteanu and Williams (2012) used WV-2 for validating the results of their glacier terrain mapping decision tree. Jawak and Luis (2011; 2013) used WV-2 for snow laden land cover mapping in Larsemann hills, Antarctica. In addition to the VHR imagery, we used elevation data via an Advanced Spaceborne Thermal Emission and Reflection Radiometer (ASTER) Global Digital Elevation Model (GDEM) v2 (spatial resolution of 30 m) to visualize a 3D surface of the study area.

Methods

The workflow developed to achieve comparative classification in this study was performed as a series of steps. These steps can be broadly distributed into four major sequences as follows; (a) image rectification and restoration, (b) object-based classification, (c) pixel-based classification, and (d) evaluation of accuracy. The methodology is illustrated in Fig. 2.

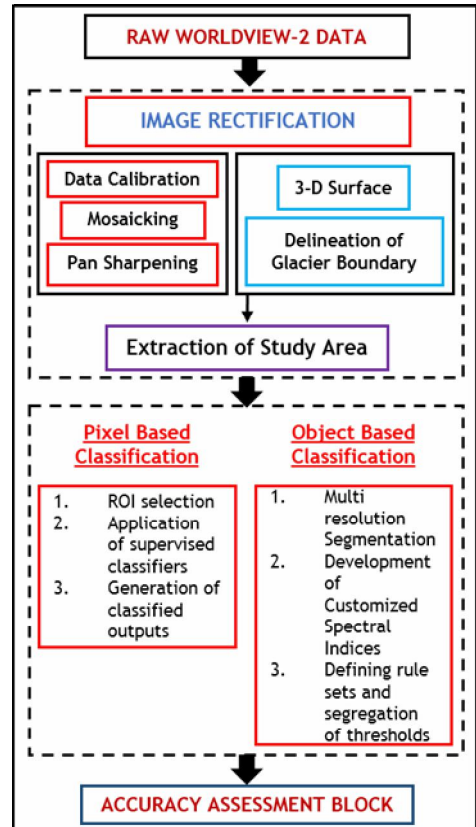


Fig. 2.►The processing chain used to preprocess and classify the images using the object-based and pixel-based classification techniques.

1. Image Rectification and Restoration

Multispectral imagery when subjected to classification necessitates a prior correction for atmospheric effects. This is especially true when techniques such as band ratioing (Paul and Hendricks 2010) involve usage of wavelengths in the visible spectrum (Cracknell and Hayes 1991). This study emphasizes the use of the characteristic spectral resolution of the WV-2 sensor to map glacier facies. Therefore, in accordance with Jawak *et al.* (2018b) the process of image rectification and restoration began by first accounting for atmospheric attenuation through data calibration. A two-step process, which includes, (a) The conversion of raw DN values to at sensor spectral radiance, followed by, (b) The conversion of at sensor radiance to at sensor or surface reflectance (Jawak and Luis 2016). The latter was carried out through the Fast Line of Sight Atmospheric Analysis of Hypercubes (FLAASH) atmospheric correction module (Kruse 2004).

The raw data was acquired as a set of

21 individual tiles (courtesy of Digital Globe©) which were then assembled through seamless mosaicking. The mosaicked imagery was then pan sharpened to enhance visual interpretation when digitizing the glacial boundaries. Among the several pan sharpening algorithms available, the Gram Schmidt (GS) pan sharpening algorithm, which is shown to be more suitable for land cover information extraction (Jawak and Luis 2013, Laben and Brower 2000) was utilized. To aid the digitization, the ASTER GDEM v2 (Tachikawa *et al.* 2011) was used to generate a 3-Dimensional (3D) surface for enhancing the topographic details (Figure 2). The final study area was then extracted and subjected to the classification protocols. The raw tiles were obtained at LV2A processing level and were orthorectified to the projection system of UTM WGS 84 43N and the geographic co-ordinate system of GCS WGS 1984. This negated the need for geometric correction.

2. Object-Based Classification

The OBC technique relies principally on the efficacy of segmentation algorithms for the creation of meaningful objects. This study applied the multiresolution segmentation algorithm as it builds upon the overall homogeneity of the generated objects (Witharana and Civco 2014). The multiresolution segmentation algorithm is a bottom-up segmentation algorithm principled on a pair-wise region merging technique ([1] - Definiens Developer 2007). This can be simply stated as an optimization procedure which divides an image into such objects that have greater homogeneity than heterogeneity. This and other segmentation algorithms can be found in software packages such as eCognition Developer, Environment of Visualizing Images (ENVI) and ERDAS IMAGINE. The characteristics of

objects generated through multiresolution segmentation depend upon certain user-defined parameters. These parameters include layer weights, scale parameter, shape and compactness. The layer weights can be thought of as levels of priority. They determine the amount of importance assigned to each spectral band in the construction of image objects. The NIR1 and NIR2 bands were given layer weights of 4 and 3, whereas, the coastal, green and red edge bands were each assigned a weightage of 2 respectively. The blue, yellow and red bands were given a weightage of 1 each. Layer weights were assigned to exploit the varying spectral properties of each band. Following recurring trials, the scale parameter was stationed at 200, the shape at 0.4 and the compactness at 0.8. Following segmen-

tation, the task of classifying the available facies was levied on the formulation of customized spectral index ratios (SIRs). The bands used to develop the customized SIRs were selected after repetitive and meticulous trials. These trials assessed the image objects and the associated spectra of identifiable facies in adherence to visual scruti-

ny and known spectral response functions. This comprehensive procedure resulted in the testing of several combinations of ratios using the selected bands. These procedures ultimately culminated into the development of three SIRs, which are listed in Table 1.

Index no.	Mathematical expression
SIR1	$\frac{(YELLOW (Band 4))}{\frac{(NIR1 (Band 7)) + (NIR2 (Band 8))}{2}}$
SIR2	$\frac{(RED EDGE (Band 6))}{\frac{(NIR1 (Band 7)) + (NIR2 (Band 8))}{2}}$
SIR3	$\frac{(BLUE (Band 2))}{\frac{(NIR1 (Band 7)) + (NIR2 (Band 8))}{2}}$

Table 1. Customized Spectral Index Ratios (SIRs) devised for mapping glacier facies in the present study.

Classification through the developed indices was performed using the rule set method. This method grants the assignation of thresholds for identifying facies. Therefore, as each threshold or multiple thresholds using one or more than one index may be used to classify the facies, it may be inferred that these thresholds are specific to that particular facies and can be used as a unique identifier for the facies un-

der consideration (Jawak et al. 2017). As observed by Jawak et al. (2018b) shadowed areas within the imagery were not easily differentiated. The spectra of shadowed regions varied both within themselves and with each other. This prohibited the existing SIRs from effectively categorizing the associated objects of the shadowed regions into a single class. Therefore, it was imperative to manually digitize shadowed regions.

3. Pixel-Based Classification

The supervised classification technique was appointed for analysing the performance of the PBC method. Three classifiers were engaged in this study, (1) Mahalanobis Distance (MHD); (2) Maximum Likelihood (MXL); and (3) Minimum Distance (MD). This PBC was performed through an extensive classification tool available in Environment of Visualizing Images (ENVI) 5.3. This tool initiates classification by the means of assessing user-provided regions

of interests (ROIs) and subsequently engaging multiple classifiers. Therefore, through a single input, multiple classified outputs can be generated. The facies thus extracted in total using both classification techniques were snow, glacier ice, ice mixed debris (IMD), debris, crevasses and shadow. The classes were identified using visual analysis of textures and tonal variations as well as spectral distinctions between the available facies.

4. Evaluation of Accuracy

In the absence of in-situ reference points, higher resolution imagery (higher in spatial/spectral resolution than the image being processed) is used to assign reference points for accuracy assessment (*e.g.* Jensen 2015). However, in the present study, the WV-2 imagery itself is of very high resolution. Therefore, due to the lack of any higher resolution imagery, sixty random points were equally assigned between each of the six classes by analysis of the spectral plots of image targets (Keshri *et al.* 2009). The spectral plots were assessed for the entire imagery to ascertain the specific signature of the target spectra. These points were then used as reference points for estimation of the accuracy through six measures derived from error matrices (Congalton and Green 2009). These measures were: (a) Error of commission (EC); (b) Error of omission (EO); (c) Producer's accuracy

(PA); (d) User's accuracy (UA); (e) Overall accuracy (OA); and (f) Kappa statistic (κ). The EC describes the total number/percentage of reference pixels incorrectly classified into a category. The EO is found when the reference pixel of a category is left out of that category in the classified output. The PA indicates the probability of the total number of pixels of that category being correctly classified. The UA delivers the probability of a pixel classified on the image truly representing that category on the ground. The OA is a percentage of the correctly classified pixels to the total pixels in the error matrix. The κ indicates the extent to which the percentage correct value of an error matrix is due to "true" agreement versus the "chance" agreement between the reference data and the classification and is calculated according to Jensen (2015).

Results

Table 2 presents the EC, EO, PA and UA derived from error matrices according to each classification scheme. The errors (EC and EO) and accuracies (PA and UA) are listed according to each facies and the average of the individual measures are calculated to simplify the analysis of the resultant errors and accuracies.

The OBC and the MD obtained a common average error of commission (EC) of 13.33%, while the MHD and MXL secured average ECs of 21.67% and 19.17% respectively (Table 2). Although it obtained the lowest EC, the MD yielded the highest average error of omission (EO) of 30.29%.

The MXL obtained an EO of 28.40%, whereas the MHD delivered an EO of 15.27% respectively. The OBC classified glacier facies with the least EO of 11.53%. Thus, having obtained the lowest errors of omission and commission (Table 2), the OBC invariably delivered the greatest pro-

ducer's accuracy (PA=88.47%) and user's accuracy (UA=86.67%).

In the PBC approach, the MHD classifier performed best, with an average PA of 80.73% and an average UA of 80.83% respectively. The MXL was the second best PBC algorithm, which obtained an average PA of 73.52% and 70.83% respectively. The MXL delivered unclassified areas solely for glacier GB. However, among all the classifiers tested, the MD performed worst, with an average PA of 68.89% and an average UA of 57.50% respectively. The three PBC methods have mapped facies for both GA and GB slightly differently. Hence, a favourable order of classification algorithms could be assigned to determine the best classifier for mapping facies. Fig. 3 illustrates the overall accuracy (OA) and the kappa statistic (κ) for the OBC and PBC classifiers tested in this study.

Thematic Class	OBC				MHD			
	Errors (%)		Accuracies (%)		Errors (%)		Accuracies (%)	
	EC	EO	PA	UA	EC	EO	PA	UA
Debris	30.00	18.06	81.94	70.00	60.00	29.29	42.14	40.00
IMD	20.00	37.50	62.50	80.00	15.00	44.37	55.63	85.00
Snow	0.00	4.55	95.45	100.00	0.00	0.00	100.00	100.00
Glacier Ice	5.00	9.09	90.91	95.00	5.00	0.00	100.00	95.00
Crevasses	25.00	0.00	100.00	75.00	30.00	13.39	86.61	65.00
Shadow	0.00	0.00	100.00	100.00	20.00	4.55	100.00	100.00
Average	13.33	11.53	88.47	86.67	21.67	15.27	80.73	80.83
Thematic Class	MXL				MD			
	Errors (%)		Accuracies (%)		Errors (%)		Accuracies (%)	
	EC	EO	PA	UA	EC	EO	PA	UA
Debris	60.00	25.00	75.00	40.00	15.00	50.00	50.00	40.00
IMD	30.00	47.53	52.47	70.00	50.00	0.00	100.00	45.00
Snow	0.00	4.55	95.45	100.00	0.00	0.00	100.00	100.00
Glacier Ice	5.00	0.00	100.00	95.00	0.00	0.00	100.00	100.00
Crevasses	20.00	36.82	63.18	65.00	0.00	69.44	8.33	5.00
Shadow	0.00	56.54	55.00	55.00	15.00	62.28	55.00	55.00
Average	19.17	28.40	73.52	70.83	13.33	30.29	68.89	57.50

Table 2. Measures of accuracy used to assess the classification accuracy in the present study. OBC: Object based classification; MHD: Mahalanobis distance; MXL: Maximum likelihood; MD: Minimum distance; EC: Error of commission; EO: Error of omission; PA: Producer’s accuracy; UA: User’s accuracy.

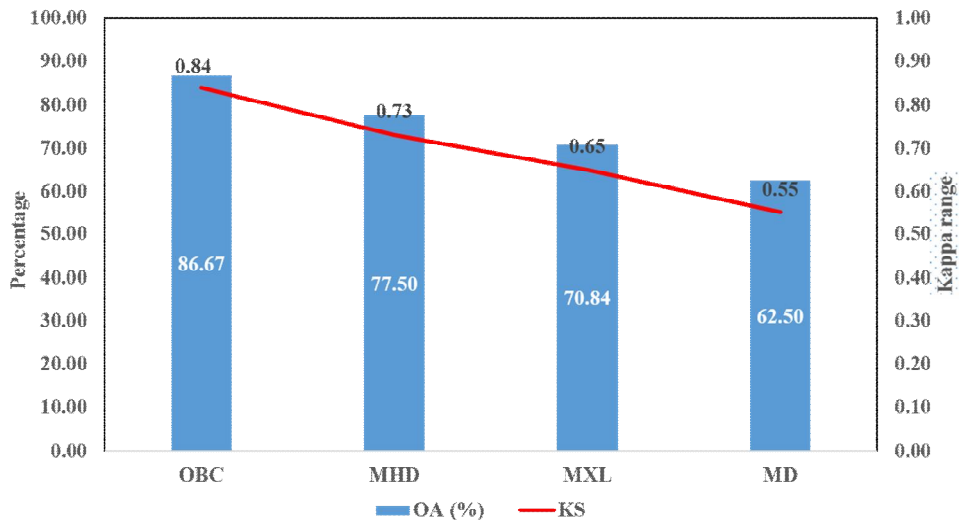


Fig. 3. Overall accuracy (OA) and Kappa statistic (KS) obtained by the Object based classification (OBC), Mahalanobis distance (MHD), Maximum likelihood (MXL), Minimum distance (MD).

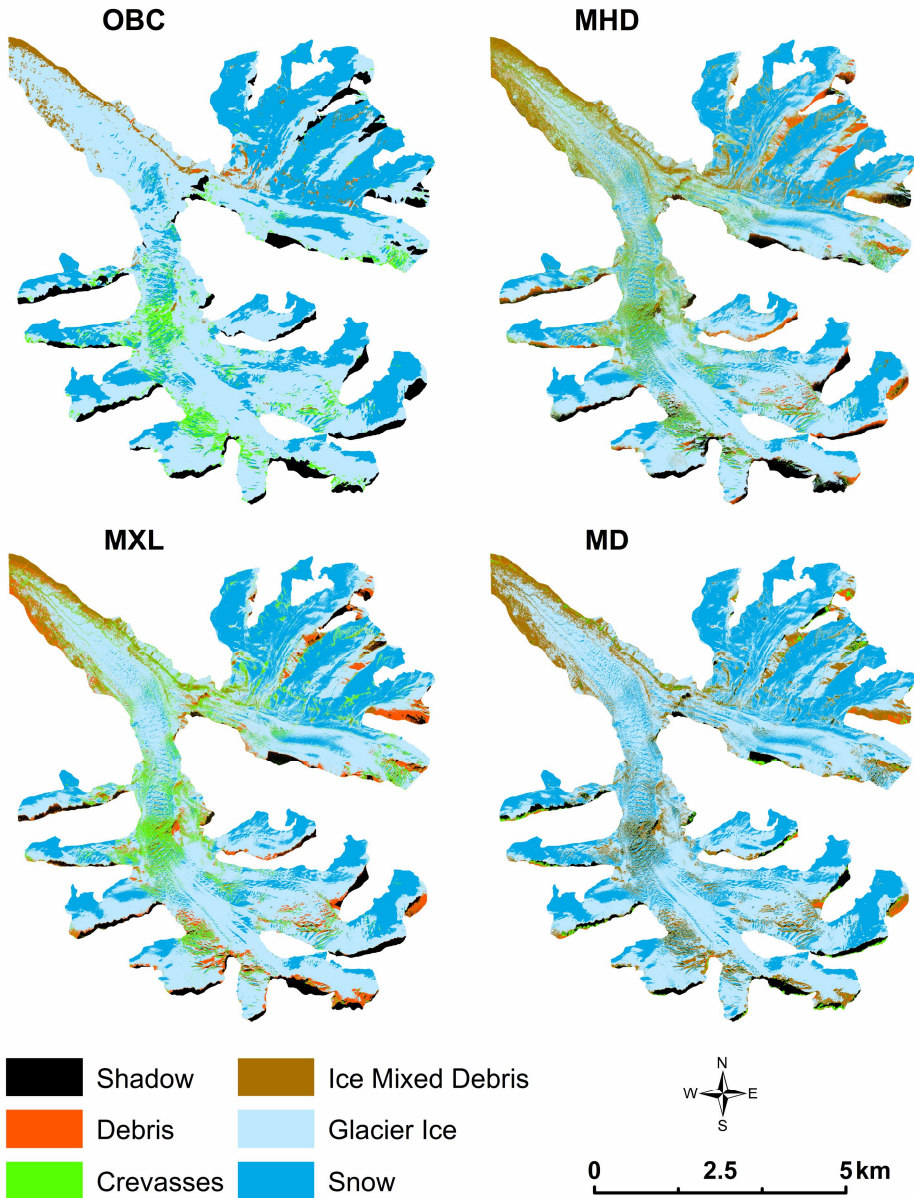


Fig. 4. Thematic classification results of GA.

The OBC was the best classifier of glacier facies with an OA of 86.67% and a kappa value of 0.84. The MD was the worst classifier in this study having delivered an OA of 62.50% and a kappa value of 0.55. The MHD is the best classifier of the PBC

method, however, it delivered a sub-average OA of 77.50% ($\kappa=0.73$). The MXL yielded an OA of 70.84% and a kappa value of 0.65. Thus, the OBC clearly outperforms the PBC methods for accurate mapping of glacier facies.

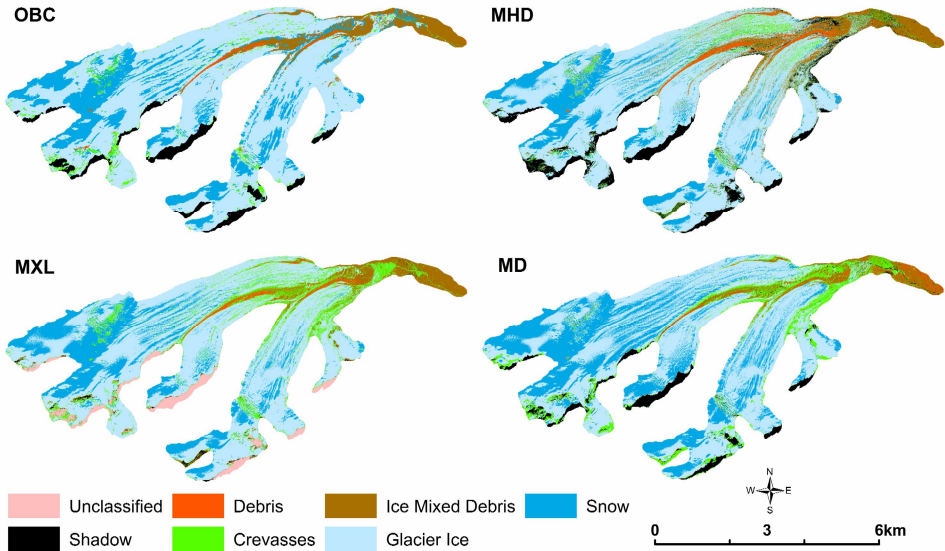


Fig. 5. Thematic classification results of GB.

Discussion

Evaluation of the spectral signature was key to identifying and building the classification schemes produced by this study. Radiometric calibration and subsequent atmospheric correction were, therefore, a crucial part of the image restorative procedure. The FLAASH atmospheric correction was selected due to its proven effectivity (Kruse 2004, Guo and Zeng 2012) and its previous tests on cryospheric regions (Jawak et al. 2018a). This permitted the multi-resolution segmentation of the OBC to characterize and isolate minute homogeneous objects. The minor differences in spectral and contextual characteristics of these objects were then burgeoned by the customized SIRs. SIR1 showed a particularly encouraging capacity for the isolation of crevasses. When paired together, SIR1 and SIR2 helped the extrication of snow and glacier ice. Neither SIR1 nor SIR2 could differentiate with certainty between IMD and debris. The chasm between these two

facies was identified solely through threshold manipulations of SIR3. An inference can be drawn from such thresholded classifications, such that as each threshold between singular and multiple indices characteristically isolates particular facies, that facies thus holds a distinct spectral response function pertaining to the spectral bands used in the concerned ratio. Such a unique function though characterized in this study through customized SIRs can be further tested in varying scenarios to identify potential applications. However, different glacial regions do not necessarily conform to identical threshold parameters. Such scenarios would require image-dependent thresholding (Bhardwaj et al. 2015, Alifu et al. 2016) to realize the full potential of the customized SIRs. Neither a single SIR, nor a combination of any of the three SIRs could isolate shadowed areas due to the spectrally complex nature of the objects created within them. In order to avoid po-

tential misclassifications, shadows were manually digitized and masked. The PBC did not need any such corrective steps. However, none of the three algorithms tested in the PBC approach could map facies with an acceptable level of accuracy. While the MHD is tested for its effectivity in glaciated regions (Jawak *et al.* 2018b, Jawak *et al.* 2017), the MXL is one of the most popularly used algorithms for classification (Shukla and Ali 2016, Khan *et al.* 2015, Sidjack 1999). However, even the MXL could not map facies with enough ac-

curacy. This reiterates the basic problems concurrent with using traditional PBC to extract information from very high-resolution imagery (Wei *et al.* 2005). Furthermore, while traditional PBC methods are faster in processing and execution and may be the preferred when a high degree of accuracy is not called for. The OBC could be preferred when accuracy is far more important than the constraint of time or when the available time is enough. Fig. 4 and Fig. 5 depict the thematic classification outputs of GA and GB.

Salient Features and Future Scope

1. Previous studies have mapped glacier facies such as snow, ice, and various debris mixed ice/snow classes using visible to short wave infrared spectral data (Pope *et al.* 2016, Pope and Rees 2014, Kulkarni *et al.* 2010, Keshri *et al.* 2009, Hall *et al.* 1988), whereas we have mapped glacier facies using only the visible to near infrared (VNIR) spectrum.

2. The distinction between debris types in satellite imagery is usually accomplished through multiple ancillary inputs (Robson *et al.* 2015, Racoviteanu and Williams 2012, Bhambri *et al.* 2011, Shukla *et al.* 2010), whereas we have segregated IMD and debris using the customized SIRs, independent of any ancillary datasets.

3. Shadowed areas presented a spectral composite of objects, which not only differed in properties within a single shadow, but also differed, within multiple shadowed regions on both the glaciers. Previous studies have indicated that greater radiometric quantization may improve the ex-

traction of shadowed areas (Gore *et al.* 2017). However, due to the lack of a higher resolution product, shadows were manually extracted.

4. While the OBC is greater in accuracy than the PBC, the former requires far more processing time than the latter. This is partly due to the semi-automated nature of the current method as well as the manual interventions. This study builds on the analysis from Jawak *et al.* (2018a, b) to apply the indices on multiple glaciers and in future studies aims to refine the present indices to function automatically, thereby reducing the manually induced temporal constraint.

5. The lack of field observations is a limiting factor at present. However, the equalized approach to sampling and accuracy assessment entail the unbiased validation. Future research will focus on in-situ validation coupled with ancillary inputs to refine the current method.

Conclusion

Classification, when emphasized on minor differences in spectral signatures, places a requisite for atmospheric corrections. The protocol followed in this study for image

restoration and rectification focuses on the derivation of relatively disturbance-free target spectra. Each step of the procedure beginning from data calibration to the extrac-

tion of the study area was performed to effectively ready the imagery for subsequent classification. The 3-dimensional surface generated through the supplementation of the ASTER GDEM not only enhanced the understanding of the terrain but also permitted topographically referenced digitization. The results generated from the OBC hold steadfast the efficiency of segmentation for extraction of fine features such as crevasses. The differences in overall accuracies do illustrate the potential applicability of such a synergistic approach of band ratioing segmented imagery to extract even the most obscure details. One of the key features of this approach is the independence of the customized SIRs from short wave infrared bands (SWIR). Glacier facies were extracted without involving SWIR wavelengths in the developed SIRs. Although the PBC did not require manual cor-

rections for its classification, the large differences in accuracy cannot be undermined. Owing to spectral complexity of the study area, a further refinement of the proposed indices is suggested for future research. SIRs developed in this study have a wider implication, however, future attempts shall be made to test the applicability and transferability of SIRs developed in the present study. Very high-resolution mapping of facies itself is rare in literature and it holds potential for mapping minor variations in facies distribution on glacier. This study demonstrates the suitability of the WV-2 VHR satellite data for effective extraction of glacier surface facies through a multi-index object-based approach. Further research is necessary to understand the nature of the specific responses to these indices as well as a test of index transferability.

References

- ALI, I., SHUKLA, A. and ROMSHOO, S. (2017): Assessing linkages between spatial facies changes and dimensional variations of glaciers in the upper Indus Basin, western Himalaya. *Geomorphology*, 284: 115-129.
- ALIFU, H., JOHNSON, B. and TATEISHI, R. (2016): Delineation of Debris Covered Glaciers Based on a Combination of Geomorphometric Parameters and a TIR/NIR/SWIR Band Ratio. *IEEE Journal of Selected Topics in Applied Earth Observations and Remote Sensing*, 9: 781-792.
- BAMBER, J. L., PAYNE, A. J. and HOUGHTON, J. (2004): Introduction and background. In: J. L. Bamber, A. J. Payne (eds.): *Mass Balance of the Cryosphere: Observations and Modelling of Contemporary and Future Changes*, Cambridge University Press: Cambridge, pp. 1-8.
- BENSON, C. (1962): Stratigraphic studies in the snow and firn of the Greenland ice sheet, Cold Regions Research and Engineering Lab Hanover, No. RR70.NH. <https://apps.dtic.mil/docs/citations/AD0288219> (accessed on 3 January 2018)
- BHAMBRI, R., BOLCH, T. and CHAUJAR, R. (2011): Mapping of debris covered glaciers in the Garhwal Himalayas using ASTER DEMs and thermal data. *International Journal of Remote Sensing*, 32: 8095-8119.
- BHARDWAJ, A., JOSHI, P., SNEHMANI, SAM, L., SINGH, M., SINGH, S. and KUMAR, R. (2015): Applicability of LANDSAT 8 data for characterizing glacier facies and supraglacial debris. *International Journal of Applied Earth Observation and Geoinformation*, 38: 51-64.
- BRAUN, M., SCHULER, T. V., HOCK, R., BROWN, I. and JACKSON, M. (2007): Comparison of remote sensing derived glacier facies maps with distributed mass balance modelling at Engabreen, northern Norway. *Proceeding Reports of the International Association of Hydrological Sciences*, 318: 126-134.
- CONGALTON, R., GREEN, K. (2009): *Assessing the Accuracy of Remotely Sensed Data: Principles and Practices*. CRC Press, Boca Raton, FL, USA. 57 p.
- CRACKNELL, A.P., HAYES, L. (1991): *Introduction to remote sensing*. Taylor & Francis, New York. pp. 222-224.

- DOZIER, J., SCHNEIDER, S. R. and MCGINNIS, D. F. (1981): Effect of grain size and snowpack water equivalence on visible and near infrared satellite observations of snow. *Water Resources Research*, 17(4):1213-1221.
- GAO, B. C., MONTES, M. J., DAVIS, C. O. and GOETZ, A. F. (2009): Atmospheric correction algorithms for hyperspectral remote sensing data of land and ocean. *Remote Sensing of Environment*, 113: S17-S24.
- GAO, Y., MAS, J. F. (2008): A comparison of the performance of pixel-based and object-based classifications over images with various spatial resolutions. *Online Journal of Earth Sciences*, 2(1): 27-35.
- GORE, A., MANI, S., SHEKHAR, C. and GANJU, A. (2017): Glacier surface characteristics derivation and monitoring using Hyperspectral datasets: A case study of Gepang Gath glacier, Western Himalaya. *Geocarto International*, 34: 23-42.
- GUO, Y., ZENG, F. (2012): Atmospheric correction comparison of SPOT-5 image based on model FLAASH and model QUAC. *International Archives of the Photogrammetry, Remote Sensing and Spatial Information Sciences*, 39(7): 21-23.
- HALL, D., CHANG, A. and SIDDALINGAIAH, H. (1988): Reflectances of glaciers as calculated using Landsat-5 Thematic Mapper data. *Remote Sensing of Environment*, 25(3): 311-321. doi: [https://doi.org/10.1016/0034-4257\(88\)90107-1](https://doi.org/10.1016/0034-4257(88)90107-1)
- HEISKANEN, J., KAJUUTTI, K., JACKSON, M., ELVEHØY, H. and PELLIKKA, P. (2002): Assessment of glaciological parameters using LANDSAT satellite data in Svartisen, northern Norway. In: *Proceedings of EARSeL-LISSIG-Workshop Observing our Cryosphere from Space*, Vol. 35.
- JAWAK, S. D., LUIS, A. J. (2011): Applications of WorldView-2 satellite data for extraction of polar spatial information and DEM of Larsemann Hills, East Antarctica. In: *International Conference on Fuzzy Systems and Neural Computing*, 3: 148-151.
- JAWAK, S. D., LUIS, A. J. (2013): Very high-resolution satellite data for improved land cover extraction of Larsemann Hills, Eastern Antarctica. *Journal of Applied Remote Sensing*, 7: 73460-73460.
- JAWAK, S. D., LUIS, A. J. (2014): A Semiautomatic Extraction of Antarctic Lake Features Using Worldview-2 Imagery. *Photogrammetric Engineering & Remote Sensing*, 80: 939-952.
- JAWAK, S. D., LUIS, A. J. (2016): Geospatial mapping of Antarctic coastal oasis using geographic object-based image analysis and high-resolution satellite imagery. In: *Proceedings of the International Society for Optics and Photonics, SPIE Asia-Pacific Remote Sensing*, 98801Q–98801Q, doi:10.1117/12.2222767
- JAWAK, S. D., WANKHEDE, S. F. and LUIS, A. J. (2017): Prospective of high-resolution WorldView-2 satellite data for geospatial surface facies mapping of an alpine glacier. In: *Proceedings of the Asian Conference on Remote Sensing*, New Delhi, India. Available online: https://a-a-r-s.org/proceeding/ACRS2017/ID_5_749/177.pdf (accessed on 02 February 2018).
- JAWAK, S. D., WANKHEDE, S. F. and LUIS, A. J. (2018a): Exploration of glacier surface facies mapping techniques using very high resolution Worldview-2 Satellite Data. *Proceedings*, 2 (7): 339. doi: <https://doi.org/10.3390/eers-2-05152>
- JAWAK, S. D., WANKHEDE, S. F. and LUIS, A. J. (2018b): Comparison of pixel and object-based classification techniques for glacier facies extraction. In: *Archives of Photogrammetry, Remote Sensing and Spatial Information Sciences*, XLII-5: 543-548, Available Online: <https://doi.org/10.5194/isprs-archives-XLII-5-543-2018>
- JENSEN, J. R. (2015): *Introductory digital image processing: a remote sensing perspective*. Prentice Hall Press, Upper Saddle River, NJ, USA, 2005, 557-580 pp.
- KESHRI, A., SHUKLA, A. and GUPTA, R. (2009): ASTER ratio indices for supraglacial terrain mapping. *International Journal of Remote Sensing*, 30: 519-524.
- KHAN, A., NAZ, B. and BOWLING, L. (2015): Separating snow, clean and debris covered ice in the Upper Indus Basin, Hindukush-Karakoram-Himalayas, using LANDSAT images between 1998 and 2002. *Journal of Hydrology*, 521: 46-64.
- KRUSE, F. A. (2004): Comparison of ATREM, ACORN, and FLAASH atmospheric corrections using low-altitude AVIRIS data of Boulder, CO. In: *Summaries of 13th JPL Airborne Geoscience Workshop*, Jet Propulsion Lab, Pasadena, CA.

- KULKARNI, A., RATHORE, B. and SINGH, S. K. (2010): Distribution of seasonal snow cover in central and western Himalaya. *Annals of Glaciology*, 51: 123-128.
- LABEN, C. A., BROWER, B. V. (2000): Process for enhancing the spatial resolution of multispectral imagery using pan-sharpening. Eastman Kodak Company, U.S. Patent 6,011,875.
- LI, M., ZANG, S., ZHANG, B., LI, S. and WU, C. (2014): A review of remote sensing image classification techniques: The role of spatio-contextual information. *European Journal of Remote Sensing*, 47(1): 389-411.
- LILLESAND, T. M., KIEFER, R. W. and CHIPMAN, J. W. (2004): Remote sensing and image interpretation. John Wiley & Sons, NJ, USA.
- PATERSON, W. S. B. (1994): The Physics of Glaciers, 3rd edn. Pergamon, Oxford.
- PAUL, F., HENDRIKS, J. (2010): Optical remote sensing of glacier extent. Remote Sensing of Glaciers: Techniques for Topographic, Spatial and Thematic Mapping of Glaciers. Taylor & Francis Group, Boca Raton, 137-152 pp.
- POPE, A., REES, G. (2014): Using in situ spectra to explore LANDSAT classification of glacier surfaces. *International Journal of Applied Earth Observation and Geoinformation*, 27: 42-52.
- POPE, E., WILLIS, I., POPE, A., MILES, E., ARNOLD, N. and REES, W. (2016): Contrasting snow and ice albedos derived from MODIS, LANDSAT ETM+ and airborne data from Langjökull, Iceland. *Remote Sensing of Environment*, 175: 183-195.
- RACOVITEANU, A., WILLIAMS, M. (2012): Decision tree and texture analysis for mapping debris-covered glaciers in the Kangchenjunga area, Eastern Himalaya. *Remote Sensing*, 4: 3078-3109.
- RASTNER, P., BOLCH, T., NOTARNICOLA, C. and PAUL, F. (2014): A comparison of pixel- and object-based glacier classification with optical satellite images. *IEEE Journal of Selected Topics in Applied Earth Observations and Remote Sensing*, 7: 853-862.
- RAUP, B. H., RACOVITEANU, A., KHALSA, S. J. S., HELM, C., ARMSTRONG, R. and ARNAUD, Y. (2007): The GLIMS geospatial glacier database: A new tool for studying glacier change. *Global and Planetary Change*, 56: 101-110. doi:10.1016/j.gloplacha.2006.07.018
- ROBSON, B., NUTH, C., DAHL, S., HÖLBLING, D., STROZZI, T. and NIELSEN, P. (2015): Automated classification of debris-covered glaciers combining optical, SAR and topographic data in an object-based environment. *Remote Sensing of Environment*, 170: 372-387.
- SHUKLA, A., ALI, I. (2016): A hierarchical knowledge-based classification for glacier terrain mapping: A case study from Kolahoi Glacier, Kashmir Himalaya. *Annals of Glaciology*, 57: 1-10.
- SHUKLA, A., ARORA, M. and GUPTA, R. (2010): Synergistic approach for mapping debris-covered glaciers using optical-thermal remote sensing data with inputs from geomorphometric parameters. *Remote Sensing of Environment*, 114: 1378-1387.
- SHUKLA, A., ARORA, M. and GUPTA, R. (2010): Synergistic approach for mapping debris-covered glaciers using optical-thermal remote sensing data with inputs from geomorphometric parameters. *Remote Sensing of Environment*, 114: 1378-1387.
- SIDJAK, R. W. (1999): Glacier mapping of the Illecillewaet icefield, British Columbia, Canada, using LANDSAT TM and digital elevation data. *International Journal of Remote Sensing*, 20: 273-284.
- TACHIKAWA, T., HATO, M., KAKU, M. and IWASAKI, A. (2011): Characteristics of ASTER GDEM version 2. In: *Proceedings of the IEEE international geoscience and remote sensing symposium*, Vancouver, Canada, 24-29 July: 3657-3660
- TSAI, Y.-L.S., DIETZ, A., OPPELT, N. and KUENZER, C. (2019): Wet and dry snow detection using Sentinel-1 SAR data for mountainous areas with a machine learning technique. *Remote Sensing*, 11: 895. doi.org/10.3390/rs11080895
- WEI, W., CHEN, X. and MA, A. (2005): Object-oriented information extraction and application in high-resolution remote sensing image. In: *Proceedings of the IEEE Geoscience and Remote Sensing Symposium*, Seoul, Korea, 29 July, 6: 3803-3806.
- WINSVOLD, S.H., KÅÅB, A. and NUTH, C. (2016): Regional glacier mapping using optical satellite data time series. *IEEE Journal of Selected Topics in Applied Earth Observations and Remote Sensing*, 9(8): 3698-3711.

- WITHARANA, C., CIVCO, D. L. (2014): Optimizing multi-resolution segmentation scale using empirical methods: Exploring the sensitivity of the supervised discrepancy measure Euclidean distance 2 (ED2). *ISPRS Journal of Photogrammetry and Remote Sensing*, 87: 108-121.
- YOUSUF, B., SHUKLA, A., ARORA, M. K. and JASROTIA, A. S. (2019): Glacier facies characterization using optical satellite data: Impacts of radiometric resolution, seasonality, and surface morphology. *Progress in Physical Geography: Earth and Environment*, 43: 473-495.
<https://doi.org/10.1177/0309133319840770>
- ZHANG, J., JIA, L., MENENTI, M. and HU, G. (2019): Glacier facies mapping using a machine-learning algorithm: The parlung Zangbo basin case study. *Remote Sensing*, 11: 452.
<https://doi.org/10.3390/rs11040452>.

Web sources / Other sources

- [1] Definiens Developer 7. (2007): Reference Book; Definiens AG: Munich, Germany. 21 p.